

Feasibility of seismic characterization of multiple fracture sets

Vladimir Grechka* and Ilya Tsvankin†

ABSTRACT

Estimation of parameters of multiple fracture sets is often required for successful exploration and development of naturally fractured reservoirs. The goal of this paper is to determine the maximum number of fracture sets of a certain rheological type which, in principle, can be resolved from seismic data. The main underlying assumption is that an estimate of the complete effective stiffness tensor has been obtained, for example, from multiazimuth, multicomponent surface seismic and vertical seismic profiling (VSP) data. Although typically only a subset of the stiffness elements (or some of their combinations) may be available, this study helps to establish the limits of seismic fracture-detection algorithms.

The number of uniquely resolvable fracture systems depends on the anisotropy of the host rock and the rheology and orientation of the fractures. Somewhat surprisingly, it is possible to characterize fewer vertical fracture sets than dipping ones, even though in the latter case the fracture dip has to be found from the data. For the simplest, rotationally invariant fractures embedded in either isotropic or transversely isotropic with a vertical symmetry axis (VTI) host rock, the stiffness tensor can be inverted for up to two vertical or four dipping fracture sets. In contrast, only one fracture set of the most general (microcorrugated) type, regardless of its orientation, is constrained by the effective stiffnesses. These results can be used to guide the development of seismic fracture-characterization algorithms that should address important practical issues of data acquisition, processing, and inversion for particular fracture models.

INTRODUCTION

Seismic fracture characterization is critically important in exploration and development of naturally fractured reservoirs which often contain multiple, differently oriented fracture net-

works (Grimm et al., 1999; Lynn et al., 1999; Pérez et al., 1999). As an example, Figure 1 shows three open fracture sets detected by a borehole imager at Weyburn field in Canada. Since all three sets may play a significant role in the fluid flow through the reservoir, it is essential to be able to resolve them using seismic methods.

According to the linear-slip theory originally suggested by Schoenberg (1980, 1983), fractures can be treated as displacement discontinuities with the jump in displacement proportional to the traction and excess fracture compliances. The compliance matrix of the effective anisotropic medium containing one or more systems of aligned fractures can be obtained by adding the compliances of each fracture set to the background compliances. Despite several limitations of the linear-slip theory (such as neglecting the interaction between fracture sets), its simplicity and generality make it particularly attractive for seismic inversion.

Since fractured reservoirs are azimuthally anisotropic, their comprehensive characterization requires acquisition of wide-azimuth, multicomponent seismic data. Processing of reflected waves produces such signatures as the NMO ellipses of different modes, amplitude variation with offset and azimuth, and shear-wave polarizations and splitting coefficients. Additionally, walkaway vertical seismic profiling (VSP) data can be used to estimate slowness surfaces and polarization vectors at receiver locations in boreholes. Available combinations of those signatures can be inverted for the effective stiffness (or compliance) coefficients of fractured rock. Then the linear-slip theory can be employed to infer the fracture compliances and orientations for a certain fracture model from the obtained stiffness (compliance) matrix. This approach is discussed in detail by Bakulin et al. (2000a,b,c, 2002), who develop practical seismic fracture-characterization algorithms for typical anisotropic models with one or two vertical fracture sets.

Estimation of fracture parameters from seismic data, however, cannot always be accomplished in a unique fashion. As noted by Bakulin et al. (2000a), it is clear that the number of fracture parameters for multiple fracture sets and low symmetries of the background rock can be much larger than 21,

Manuscript received by the Editor June 20, 2002; revised manuscript received February 18, 2003.

*Formerly Colorado School of Mines, Center for Wave Phenomena, Golden, Colorado 80401; presently Shell International Exploration and Production Inc., Bellaire Technology Center, 3737 Bellaire Blvd., Houston, Texas 77001-0481.

†Colorado School of Mines, Center for Wave Phenomena, Department of Geophysics, Golden, Colorado 80401-1887. E-mail: ilya@dix.mines.edu.

© 2003 Society of Exploration Geophysicists. All rights reserved.

the maximum possible number of independent stiffness coefficients describing wave propagation in the effective fractured medium. Hence, there exists a finite subset of fractured models (with a relatively small number of fracture sets) which can be unambiguously characterized based on seismic data. In fact, the class of such resolvable fractured models is limited not just by the number of unknown fracture parameters. Elaborate analysis of the stiffness tensor shows that certain compliances of differently oriented fracture sets may contribute to the same effective stiffness coefficient (e.g., Bakulin et al., 2002). As a result, it is possible to resolve only particular combinations of those compliances rather than their individual values.

The goal of this paper is to identify fracture sets whose compliances and orientations can be determined (in principle) from seismic data. We examine three different rheological types of fractures—rotationally invariant, diagonal [called orthotropic by Schoenberg and Helbig (1997)], and completely general (Grechka et al., 2003; a description of all three types is given below). The fractures are embedded in either isotropic or transversely isotropic with a vertical symmetry axis (VTI) host rock, with each fracture set arbitrarily oriented in 3D space. Throughout the paper, we assume an ideal scenario when all 21 stiffness coefficients have been estimated, for example, from multiazimuth walkaway P- and S-wave VSP data or from a combination of surface and VSP data (e.g., Bakulin et al., 2000d; Horne and Leaney, 2000; Grechka et al., 2001; Dewangan and Grechka, 2002). By computing the Fréchet derivatives of the effective stiffness coefficients with respect to the fracture and background parameters, we determine how many different fracture sets of a certain type (along with the unknown background parameters) are constrained by the stiffness matrix. This analysis reveals the dependence of the maximum number of resolvable fracture sets on the rheology

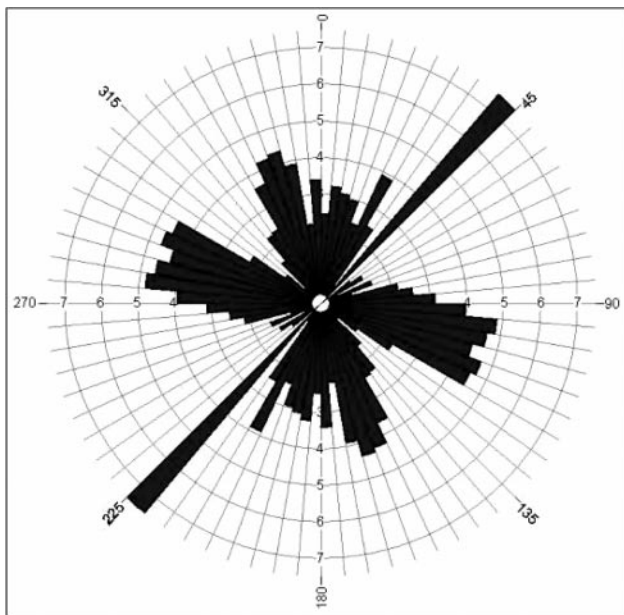


FIG. 1. Rose diagram of open-fracture azimuths obtained by a borehole imager at Weyburn field (Canada). The plot is courtesy of the Reservoir Characterization Project at Colorado School of Mines.

and orientation of the fractures, as well as on the presence of anisotropy in the background.

EFFECTIVE STIFFNESS OF FRACTURED ROCK

General relationships

According to the linear-slip theory (Schoenberg, 1980, 1983; Nichols et al., 1989; Schoenberg and Muir, 1989; Schoenberg and Sayers, 1995), the effective compliance matrix \mathbf{s} of a medium containing N sets of aligned fractures is given by

$$\mathbf{s} = \mathbf{s}_b + \sum_{i=1}^N \mathbf{s}_f^{(i)}, \quad (1)$$

where \mathbf{s}_b and $\mathbf{s}_f^{(i)}$ are the 6×6 symmetric compliance matrices of the unfractured background and the i th fracture set, respectively. By definition, the effective stiffness matrix \mathbf{c} is the inverse of the compliance matrix:

$$\mathbf{c} = \mathbf{s}^{-1} = \left(\mathbf{s}_b + \sum_{i=1}^N \mathbf{s}_f^{(i)} \right)^{-1} = \left(\mathbf{c}_b^{-1} + \sum_{i=1}^N \mathbf{s}_f^{(i)} \right)^{-1}; \quad (2)$$

\mathbf{c}_b is the stiffness matrix of the host (background) rock. Note that all inverse matrices used here exist because the background matrices \mathbf{c}_b and \mathbf{s}_b are positive definite and the compliance matrices $\mathbf{s}_f^{(i)}$ are nonnegative definite.

Here, we examine two types of the host rock: isotropic (denoted as ISO) and VTI. Using the Lamé parameters λ and μ , the isotropic stiffness matrix can be written as

$$\mathbf{c}_b^{\text{ISO}} = \begin{pmatrix} \lambda + 2\mu & \lambda & \lambda & 0 & 0 & 0 \\ \lambda & \lambda + 2\mu & \lambda & 0 & 0 & 0 \\ \lambda & \lambda & \lambda + 2\mu & 0 & 0 & 0 \\ 0 & 0 & 0 & \mu & 0 & 0 \\ 0 & 0 & 0 & 0 & \mu & 0 \\ 0 & 0 & 0 & 0 & 0 & \mu \end{pmatrix}. \quad (3)$$

For VTI media, the stiffness matrix has the form

$$\mathbf{c}_b^{\text{VTI}} = \begin{pmatrix} c_{11b} & c_{12b} & c_{13b} & 0 & 0 & 0 \\ c_{12b} & c_{11b} & c_{13b} & 0 & 0 & 0 \\ c_{13b} & c_{13b} & c_{33b} & 0 & 0 & 0 \\ 0 & 0 & 0 & c_{44b} & 0 & 0 \\ 0 & 0 & 0 & 0 & c_{44b} & 0 \\ 0 & 0 & 0 & 0 & 0 & c_{66b} \end{pmatrix}, \quad (4)$$

where $c_{12b} = c_{11b} - 2c_{66b}$.

The matrices $\mathbf{c}_b^{\text{ISO}}$ and $\mathbf{c}_b^{\text{VTI}}$ are written in a certain global Cartesian coordinate frame $\{x_1, x_2, x_3\}$ used to describe both the background and the embedded fractures. Whereas the orientation of this frame can be arbitrary for isotropic host rock, in the case of the VTI background the x_3 -axis is taken parallel to the symmetry axis of the medium.

Excess fracture compliance

The excess compliance of a fracture set of the most general rheological type with the normal in the x_1 -direction is described

by the following 6×6 symmetric matrix (Schoenberg, 1980; Bakulin et al., 2000c; Grechka et al., 2001):

$$\mathbf{s}_f^{\text{GN},x_1} = \begin{pmatrix} K_N & 0 & 0 & 0 & K_{NV} & K_{NH} \\ 0 & 0 & 0 & 0 & 0 & 0 \\ 0 & 0 & 0 & 0 & 0 & 0 \\ 0 & 0 & 0 & 0 & 0 & 0 \\ K_{NV} & 0 & 0 & 0 & K_V & K_{VH} \\ K_{NH} & 0 & 0 & 0 & K_{VH} & K_H \end{pmatrix}. \quad (5)$$

The diagonal elements of the matrix $\mathbf{s}_f^{\text{GN},x_1}$ are responsible for the normal (K_N) and tangential (K_V and K_H) compliances of the fracture. The nonzero off-diagonal elements (K_{NV} , K_{NH} , and K_{VH}) imply the existence of coupling between the normal (to the fracture plane) traction and the tangential jump in displacement (displacement discontinuity is often called slip). Likewise, tangential traction components for general fractures are coupled to normal slips. This coupling may be caused by microcorrugation of fracture surfaces (Schoenberg and Douma, 1988; Grechka et al., 2001) or misalignment of the fracture strike and the principal axes of stress (Nakagawa et al., 2000).

It can be shown (Berg et al., 1991) that any rotation of the fracture plane around the x_1 -axis does not change the form of the matrix $\mathbf{s}_f^{\text{GN},x_1}$. However, if the fracture normal deviates from the x_1 -axis, the excess fracture compliance matrix $\mathbf{s}_f^{\text{GN},n}$ may no longer contain any vanishing elements. We describe the fracture normal \mathbf{n} by its azimuth α and dip (or tilt) β (Figure 2):

$$\mathbf{n} = \{\cos \alpha \cos \beta, \sin \alpha \cos \beta, -\sin \beta\}. \quad (6)$$

Exact expressions for the elements of the matrix $\mathbf{s}_f \equiv \mathbf{s}_f^{\text{GN},n}$ in terms of the angles α and β are given in Appendix A [equations (A-4)–(A-24)]. Those equations are essential for the problem at hand because they represent the most general excess fracture compliance matrix allowed by the linear-slip theory. The compliance matrices for fracture sets with any par-

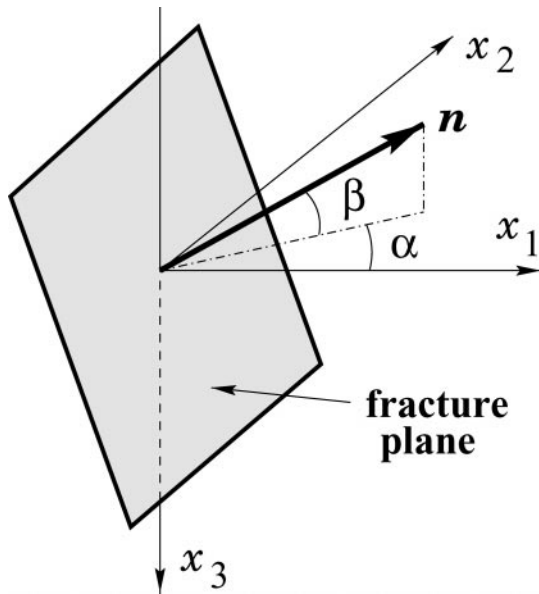


FIG. 2. Orientation of a fracture set is defined by the azimuth α and dip β of the unit vector \mathbf{n} orthogonal to the fracture plane.

ticular rheology or orientation can be obtained as special cases of the matrix \mathbf{s}_f . For instance, equations (2) of Schoenberg et al. (1999) for vertical fractures with a diagonal compliance matrix follow from equations (A-4)–(A-24) by simply setting $K_{NV} = K_{NH} = K_{VH} = 0$ and $\beta = 0$.

For fractures with a less complicated rheology, normal tractions are decoupled from tangential slips, and tangential tractions are decoupled from normal slips. Then, in a certain coordinate frame the excess fracture compliance matrix (5) becomes diagonal. Therefore, we call fractures of this type diagonal and denote them with the superscript DI. It should be noted, however, that the compliance matrix $\mathbf{s}_f^{\text{DI},x_1}$ of diagonal fractures acquires a nonzero off-diagonal element s_{56f}^{DI,x_1} after an arbitrary rotation around the fracture normal (i.e., the x_1 -axis). Thus, the compliance matrix of diagonal fractures is given by

$$\mathbf{s}_f^{\text{DI},x_1} = \begin{pmatrix} K_N & 0 & 0 & 0 & 0 & 0 \\ 0 & 0 & 0 & 0 & 0 & 0 \\ 0 & 0 & 0 & 0 & 0 & 0 \\ 0 & 0 & 0 & 0 & 0 & 0 \\ 0 & 0 & 0 & 0 & K_V & K_{VH} \\ 0 & 0 & 0 & 0 & K_{VH} & K_H \end{pmatrix}. \quad (7)$$

To make the matrix $\mathbf{s}_f^{\text{DI},x_1}$ diagonal, the coordinate frame has to be rotated by the angle $\nu = (1/2) \tan^{-1} [2 K_{VH} / (K_V - K_H)]$ around the x_1 -axis. Equations (A-4)–(A-24) of Appendix A yield the compliance matrix of diagonal fractures orthogonal to the vector \mathbf{n} [equation (6)] if one substitutes

$$K_{NV} = K_{NH} = 0. \quad (8)$$

The simplest type of fractures, called rotationally invariant (RI in our notation) by Schoenberg and Sayers (1995), corresponds to diagonal fractures with equal tangential compliances $K_V = K_H$ (then $K_{VH} = 0$):

$$\mathbf{s}_f^{\text{RI},x_1} = \begin{pmatrix} K_N & 0 & 0 & 0 & 0 & 0 \\ 0 & 0 & 0 & 0 & 0 & 0 \\ 0 & 0 & 0 & 0 & 0 & 0 \\ 0 & 0 & 0 & 0 & 0 & 0 \\ 0 & 0 & 0 & 0 & K_V & 0 \\ 0 & 0 & 0 & 0 & 0 & K_V \end{pmatrix}. \quad (9)$$

Any rotation around the fracture normal (i.e., around the x_1 -axis) does not change the form of the matrix (9). Hence, the compliance $\mathbf{s}_f^{\text{RI},n}$ of a rotationally invariant fracture set with the normal \mathbf{n} can be found from equations (A-4)–(A-24) after the following substitutions:

$$K_{NV} = K_{NH} = K_{VH} = 0 \quad \text{and} \quad K_H = K_V. \quad (10)$$

Table 1 lists the number of independent physical model parameters for the two types of host rock (background) and three types of fracture systems considered above. The dimension of the composite parameter space for the effective model is equal to the sum of the dimensions of the individual parameter spaces. For example, the medium formed by two rotationally

invariant fracture sets embedded in a purely isotropic background is described by a total of $(2 \times 4) + 2 = 10$ independent parameters.

Since fracture characterization can be unique only if there are no more than 21 physical parameters (the number of stiffness coefficients for the most general, triclinic symmetry), Table 1 helps to identify fractured models that cannot (even in principle) be constrained by seismic data. For instance, it is impossible to estimate the parameters of three arbitrarily oriented diagonal fracture sets in a VTI host rock because the total number of parameters in this case is $(3 \times 6) + 5 = 23$ which is greater than 21.

FRECHÈT DERIVATIVES OF THE EFFECTIVE STIFFNESS MATRIX

Although Table 1 provides useful insight into the fracture-characterization problem, it only shows that for a certain class of models the number of constraints is smaller than the number of unknowns, so the fracture and background parameters cannot be resolved. However, even if the number of effective stiffness coefficients is larger than the number of unknown physical parameters, the inversion for a particular parameter can still be ambiguous.

To study the uniqueness of this nonlinear inverse problem, we apply the singular value decomposition (SVD) to the matrix of Frechét derivatives of the effective stiffnesses \mathbf{c} with respect to the model parameters. The model parameter vector \mathbf{m} can be represented as

$$\mathbf{m} \equiv \mathbf{b} \cup \mathbf{f}^{(1)} \cup \dots \cup \mathbf{f}^{(N)}. \quad (11)$$

Here, the vector \mathbf{b} contains the independent background stiffness coefficients \mathbf{c}_b ; for instance, $\mathbf{b} = [b_1, b_2] = [\lambda, \mu]$ when the host rock is isotropic. Similarly, the vectors $\mathbf{f}^{(1)}, \dots, \mathbf{f}^{(N)}$ are composed of the independent excess fracture compliances \mathbf{s}_f [equations (5), (7), or (9)] and the orientation angles of each fracture set. Note that even though the elements of \mathbf{c}_b and \mathbf{s}_f are conventionally written in the form of 6×6 matrices, we include them in the single vector \mathbf{m} to calculate the Frechét derivatives.

As discussed above, the necessary prerequisite for a unique inversion is

$$\dim \mathbf{m} = \dim \mathbf{b} + \sum_{i=1}^N \dim \mathbf{f}^{(i)} \leq 21, \quad (12)$$

where $\dim \mathbf{v}$ denotes the dimension of each vector \mathbf{v} . The matrix of Frechét derivatives can be obtained by differentiating

Table 1. Number of independent parameters needed to describe isotropic (ISO) and VTI background media, as well as rotationally invariant (RI), diagonal (DI), and general (GN) fractures. The numbers for each fracture set include the independent compliances and orientation angles α and β .

Host rock		Fracture set		
ISO	VTI	RI	DI	GN
2	5	4	6	8

equation (2):

$$\begin{aligned} \mathcal{F} &\equiv \frac{\partial \mathbf{c}}{\partial \mathbf{m}} = \frac{\partial}{\partial \mathbf{m}} \left[\left(\mathbf{c}_b^{-1} + \sum_{i=1}^N \mathbf{s}_f^{(i)} \right)^{-1} \right] \\ &= - \left(\mathbf{c}_b^{-1} + \sum_{i=1}^N \mathbf{s}_f^{(i)} \right)^{-1} \left(-\mathbf{c}_b^{-1} \frac{\partial \mathbf{c}_b}{\partial \mathbf{m}} \mathbf{c}_b^{-1} + \sum_{i=1}^N \frac{\partial \mathbf{s}_f^{(i)}}{\partial \mathbf{m}} \right) \\ &\quad \times \left(\mathbf{c}_b^{-1} + \sum_{i=1}^N \mathbf{s}_f^{(i)} \right)^{-1}. \end{aligned} \quad (13)$$

Applying equation (2) again yields

$$\begin{aligned} \mathcal{F} &= \mathbf{c} \left(\mathbf{c}_b^{-1} \frac{\partial \mathbf{c}_b}{\partial \mathbf{m}} \mathbf{c}_b^{-1} - \sum_{i=1}^N \frac{\partial \mathbf{s}_f^{(i)}}{\partial \mathbf{m}} \right) \mathbf{c} \\ &= \mathbf{c} \left(\mathbf{s}_b \frac{\partial \mathbf{c}_b}{\partial \mathbf{m}} \mathbf{s}_b - \sum_{i=1}^N \frac{\partial \mathbf{s}_f^{(i)}}{\partial \mathbf{m}} \right) \mathbf{c}. \end{aligned} \quad (14)$$

Note that all derivatives in equation (14) are easy to find in explicit form because the stiffness matrix \mathbf{c}_b is differentiated only with respect to the stiffness coefficients of the host rock [i.e., to the portion \mathbf{b} of the vector \mathbf{m} ; see equation (11)], while the compliance matrices $\mathbf{s}_f^{(i)}$ are differentiated only with respect to the fracture compliances and orientations (i.e., to the portions $\mathbf{f}^{(i)}$ of \mathbf{m}). Indeed, \mathbf{c}_b is independent of $\mathbf{s}_f^{(i)}$, so the corresponding derivative $\partial \mathbf{c}_b / \partial \mathbf{f}^{(i)} = 0$ for any i ; likewise, $\partial \mathbf{s}_f^{(i)} / \partial \mathbf{b} = 0$ and, if $i \neq j$, $\partial \mathbf{s}_f^{(i)} / \partial \mathbf{f}^{(j)} = 0$. Clearly, the Frechét matrix \mathcal{F} , which has the dimension $21 \times \dim \mathbf{m}$, is sparse because so many derivatives in equation (14) vanish.

ANALYSIS OF THE FRECHÈT MATRIX

To answer the question whether it is possible to estimate the parameter vector \mathbf{m} from the measured stiffness coefficients \mathbf{c} , we perform SVD of the matrix \mathcal{F} . According to the standard SVD criterion, if the condition number κ (defined as the ratio of the greatest singular value to the smallest one) of \mathcal{F} is finite,

$$\kappa \equiv \text{cond } \mathcal{F} < \infty, \quad (15)$$

the inversion for \mathbf{m} is theoretically unique (for noise-free data). Estimation of \mathbf{m} becomes ambiguous (nonunique) if

$$\kappa = \infty. \quad (16)$$

To identify the maximum possible number of fracture sets which can be resolved using the effective stiffness coefficients, we use the following simple approach. After choosing the symmetry of the host rock (isotropic or VTI), we keep adding fracture sets of a certain type to the model until the condition number becomes infinite. In the tests below, κ is considered infinite if it exceeds the numerical limit set in the Matlab software ($2^{210} \approx 1.8 \times 10^{308}$).

Arbitrarily oriented (dipping) fractures

The analysis of the condition number for fracture sets with arbitrary dip and azimuth is summarized in Table 2. The results show an intuitively obvious trend: the more complicated the rheology of the fracture systems, the fewer such systems can

be uniquely estimated from the effective stiffnesses. It is interesting that for rotationally invariant and diagonal fractures, it should be possible to invert for as many fracture sets as allowed by the dimensionality constraint (12). In contrast, the stiffness matrix can be inverted for the parameters of only one general fracture set, even for the simplest isotropic background rock.

Obviously, a finite value of the condition number indicates the possibility of inverting a complete, 21-element stiffness matrix for the medium parameters. Estimating the stiffness matrix itself is a highly challenging problem that typically requires acquisition and processing of multicomponent, multiazimuth data. Despite a significant progress recently achieved in the inversion for transversely isotropic (e.g., Bakulin et al., 2000a; Horne and Leaney, 2000; Tsvankin and Grechka, 2000a,b; Tsvankin, 2001; Grechka et al., 2002), orthorhombic (Grechka et al., 1999; Bakulin et al., 2000b), monoclinic (Bakulin et al., 2000c; Grechka et al., 2000) and even triclinic (Grechka et al., 2003; Dewangan and Grechka, 2002) media, parameter estimation for lower anisotropic symmetries requires further development.

In particular, seismic signatures needed for characterization of dipping fractures have seldom been discussed in the literature. An interesting possibility explored in the work of Angerer et al. (2002) is to use reflection traveltimes of mode-converted PS-waves in the detection of fracture dip. The presence of dipping fractures in an otherwise laterally homogeneous, isotropic background medium makes PS traveltime asymmetric with respect to the source and receiver locations (i.e., the traveltime does not remain the same if one interchanges the source and receiver). Angerer et al. (2002) introduce a measure of this traveltime asymmetry that can be inverted for the fracture dip and apply their methodology to 3D multicomponent data from the Emilio field in the Adriatic Sea.

A relatively simple model with a single set of dipping rotationally invariant fractures in a VTI host rock (marked by a diamond in Table 2) is analyzed by Grechka and Tsvankin (2003). The effective medium in this case has monoclinic symmetry with a vertical symmetry plane that coincides with the dip plane of the fractures. Grechka and Tsvankin (2003) show that all fracture and background parameters can be obtained from the vertical velocities and NMO ellipses of PP-waves and two split SS-waves (SS traveltimes can be obtained from PP and PS data; see Grechka and Tsvankin, 2002) reflected from horizontal interfaces.

The analysis of the Fréchet derivatives indicates that it is possible to resolve a total of four systems of rotationally invariant fractures in a VTI background. Such a model has the maximum possible number of independent physical parameters (21), all of which can be estimated from the stiffness matrix of the effective triclinic medium.

Table 2. Maximum number of dipping fracture sets that can be uniquely resolved from the error-free stiffness matrix. The diamond marks the model studied by Grechka and Tsvankin (2003).

	RI	DI	GN
ISO	4	3	1
VTI	4 [♦]	2	1

Figure 3 shows a typical example of the relationship between the condition number κ and the dip β of the fracture normal (i.e., β is the fracture tilt away from the vertical; see Figure 2) for a model that includes three rotationally invariant fracture sets. For a wide range of dips, the curve is almost flat with finite values of κ , which indicates that the inverse problem is well posed (according to our criterion). Although the condition number for the flat part of the curve is relatively large ($10^2 < \kappa < 10^3$), our previous results (Bakulin et al., 2000a,b,c) indicate that parameter estimation for some models with κ of such magnitude is not only theoretically possible but also sufficiently stable in the presence of errors in the data.

Only for values of β extremely close to 0° (near-vertical fractures) and 90° (near-horizontal fractures) does the condition number rapidly go to infinity. The parameter-estimation problem for vertical fractures is discussed in detail in the next section. Horizontal fractures are not typical for naturally fractured reservoirs and will not be analyzed further.

Vertical fractures

Most existing papers on fracture characterization treat vertical fracture networks, which are believed to be common for naturally fractured reservoirs. To establish the maximum number of vertical fracture sets that can be characterized by seismic data, we set the fracture tilt β (Figure 2) to zero and assume that it is known a priori. Although it seems that making the fractures vertical should help in fracture detection because each set is described by one fewer parameter, Table 3 proves this expectation to be wrong. For instance, for rotationally invariant fractures in both isotropic and VTI background, the maximum number of resolvable vertical sets is just two compared to four dipping sets in Table 2.

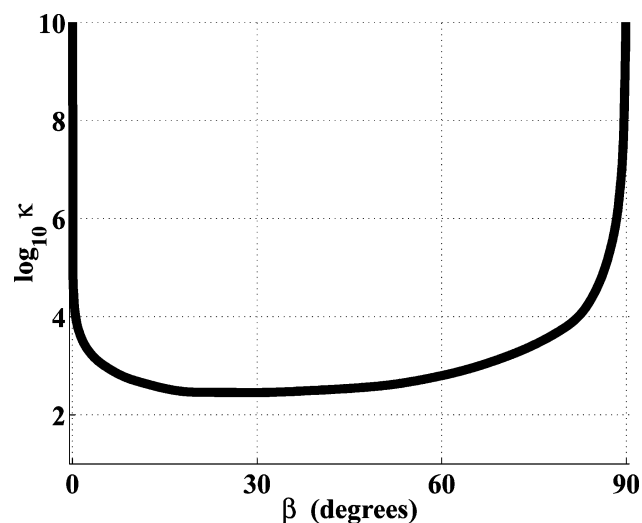


FIG. 3. The influence of the dip β of the fracture normal on the condition number κ of the Fréchet matrix. The model includes three rotationally invariant fracture sets with the same β embedded in isotropic rock with $V_P/V_S = 2$ ($\beta = 0^\circ$ corresponds to vertical fractures). For the first set, $K_N^{(1)} = 0.11$ (all compliances are density normalized and given in s^2/km^2), $K_V^{(1)} = 0.18$, and $\alpha^{(1)} = 0^\circ$ (α is the azimuth of the fracture normal); for the second set, $K_N^{(2)} = 0.15$, $K_V^{(2)} = 0.13$, and $\alpha^{(2)} = 60^\circ$; for the third set, $K_N^{(3)} = 0.16$, $K_V^{(3)} = 0.19$, and $\alpha^{(3)} = 120^\circ$.

To explain this puzzling result, note that making the fractures vertical ($\beta = 0$) removes one degree of freedom in the description of each fracture set. As a consequence, certain excess compliances of different fracture systems can map into the same element of the effective stiffness matrix, which makes estimation of these individual compliances impossible. An example of this type of ambiguity is discussed by Bakulin et al. (2002) for two orthogonal vertical fracture sets in a VTI host rock (see below).

The simplest fractured model is that of vertical rotationally invariant fractures in an otherwise isotropic host rock (one star in Table 3). For a single fracture set, the effective medium is transversely isotropic with a horizontal symmetry axis (e.g., Schoenberg and Sayers, 1995; Bakulin et al., 2000a). Fracture-characterization algorithms for this model (see Bakulin et al., 2000a) can be based entirely on surface reflection data. Two vertical fracture systems making an arbitrary angle with each other lower the effective medium symmetry to monoclinic (the only symmetry plane of this model is horizontal). In the special cases of orthogonal or identical fracture sets, the effective model is orthorhombic. For both orthorhombic and monoclinic models with two vertical fracture sets, the fracture and background parameters can be estimated using the vertical velocities and NMO ellipses of PP- and two split SS-waves (or converted PS-waves) from horizontal interfaces (Bakulin et al., 2000b,c).

Two vertical, rotationally invariant fracture sets in a VTI background (two stars in Table 3) also yield an effective monoclinic medium with a horizontal symmetry plane. Bakulin et al. (2002) show that if the fracture sets are orthogonal (then the effective medium is orthorhombic), the fracture and background parameters cannot be estimated in a unique fashion. Although the number of the physical parameters in this model is equal to the number of nonzero effective stiffnesses (nine), there is an additional relation (constraint) between the stiffnesses or Tsvankin's (1997) anisotropic coefficients that causes the ambiguity.

While this conclusion is correct, our study reveals that the orthogonal orientation of the fracture systems is the only special case for this model when the Frechét matrix \mathcal{F} degenerates. As illustrated by Figure 4, the condition number κ rapidly increases only when the angle $\Delta\alpha$ between the fractures is in a narrow vicinity of 0° (parallel sets) or 90° (orthogonal sets). Even if $\Delta\alpha$ deviates by just a few degrees from 90° , the inversion should be feasible, and the stiffnesses of the effective monoclinic medium (this model is similar to the one described by Bakulin et al., 2000c) can be used to constrain the fracture and background parameters.

A single system of vertical diagonal fractures [equation (7)] with $K_{VH} = 0$ in a VTI host rock (one dagger in Table 3) creates an effective orthorhombic medium (Schoenberg and Helbig, 1997). Bakulin et al. (2000b) show that the fracture compliances and orientations for this model can be estimated

Table 3. Maximum number of vertical fracture sets that can be uniquely resolved from the error-free stiffness matrix. The stars and daggers mark models studied in the literature (see the main text).

	RI	DI	GN
ISO	2*	2	1 [†]
VTI	2**	2 [†]	1

from multiazimuth PP and PS (or SS) reflection data, although one of the tangential compliances (K_H) remains unconstrained if dipping events are not available. The inversion for the VTI background parameters also requires knowledge of the vertical velocities or reflector depth. Moreover, Table 3 indicates that the parameter estimation is still possible for two sets of diagonal fractures in both isotropic and VTI background. The compliances of two fracture sets, however, cannot be determined without using multiazimuth VSP data.

Characterization of vertical fractures of the most general type embedded in a purely isotropic host rock (dagger in Table 3) has been studied by Grechka et al. (2003). Despite the lowest possible (triclinic) symmetry of the effective model, Grechka et al. (2003) prove that the fracture and background parameters can be determined from a combination of reflection and borehole data that includes the vertical velocities and NMO ellipses of PP- and SS-waves supplemented with P-wave multiazimuth walkaway VSP data. According to Table 3, the addition of another general fracture system makes the inversion ambiguous, although the number of independent physical parameters for either (isotropic or VTI) background still does not exceed 21.

DISCUSSION AND CONCLUSIONS

Seismic estimation of the parameters of multiple fracture sets embedded in otherwise isotropic or VTI background (host) rock is an important practical issue in characterization and development of naturally fractured reservoirs. Although our approach can be applied to other types of host rock (i.e., orthorhombic or monoclinic), such low background symmetries can be caused only by the intrinsic anisotropy of the rock-forming crystals. Since crystal anisotropy is known to be atypical for relatively shallow strata important in seismic exploration, we decided to exclude those more complicated background models from consideration.

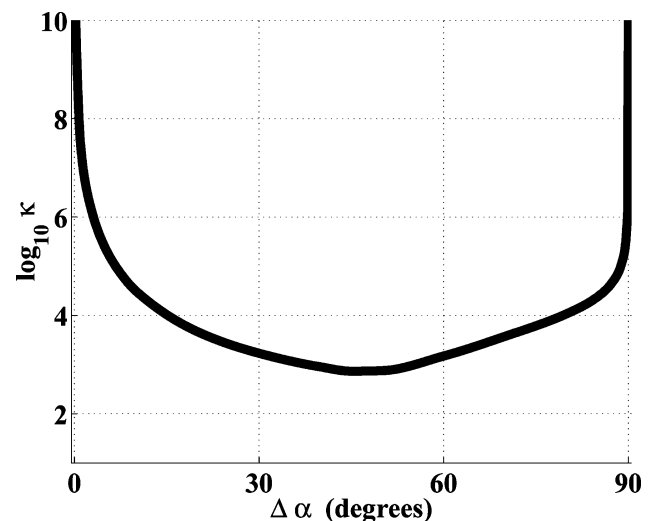


FIG. 4. The condition number κ for the model of two vertical, rotationally invariant fracture sets in VTI host rock. $\Delta\alpha$ denotes the difference between the fracture azimuths. The compliances are $K_N^{(1)} = 0.15$, $K_V^{(1)} = 0.14$, $K_N^{(2)} = 0.13$, and $K_V^{(2)} = 0.12$. The density-normalized background stiffnesses (in km^2/s^2) are $c_{11} = 3.90$, $c_{33} = 4.00$, $c_{44} = 1.00$, $c_{66} = 1.19$, and $c_{13} = 1.71$.

The key assumption in our study was that all elements of the effective stiffness matrix \mathbf{c}_{ij} can be recovered from seismic data. By expressing the stiffnesses through the fracture and background parameters and analyzing the condition number of the corresponding Fréchet matrix, we determined the maximum number of fracture sets with a given rheology which can be uniquely resolved under those ideal conditions. If the fracture sets are tilted away from the vertical (i.e., the fractures are dipping), it may be possible to characterize up to four rotationally invariant fracture sets in either isotropic or VTI background. Surprisingly, parameter estimation becomes more ambiguous for vertical fractures which create simpler (i.e., higher-symmetry) effective anisotropic models. Because of the trade-offs between different fracture parameters which contribute to the effective stiffnesses only in certain combinations, no more than two vertical fracture sets can be resolved from the matrix \mathbf{c}_{ij} . Even a small fracture dip, however, is sufficient to sharply reduce the condition number and make the inverse problem much better posed.

In practice, estimation of fracture parameters has to be based on available (incomplete) data which usually cannot constrain all stiffness coefficients individually. This is particularly true for lower anisotropic symmetries (such as triclinic) described by up to 21 independent stiffnesses. Inversion of field data may yield only combinations of some stiffness elements, while information about other stiffnesses may be missing entirely. Such an incomplete stiffness matrix may constrain fewer fracture sets than indicated by our analysis (if any), so it may become necessary to impose restrictions on the fracture rheology (e.g., assume rotationally invariant fractures) and orientation, or ignore the background anisotropy. In principle, a feasibility study similar to the one described here can be carried out for any given set of available seismic data or effective stiffness coefficients.

Another reason for our results to be overly optimistic is that we deem the inversion to be nonunique only when the condition number of the Fréchet matrix goes to infinity. Therefore, the entries in Tables 2 and 3 formulated in a yes/no fashion should be regarded with caution. For the vast transitional set of models with relatively large condition numbers, the feasibility of inversion depends on the magnitude of errors in the data. As an example, according to the view taken in our paper, two fracture sets making a small angle with each other may still be resolvable if the corresponding condition number is finite (see Figure 4). However, this is not necessarily the case in practice, when the effective stiffness coefficients are estimated with an error. It is clear from both the physics and mathematics of the linear-slip theory that if the angle between two fracture sets is smaller than a certain value (which depends on errors in c_{ij}), they appear as a single set with the total excess compliance equal to the sum of the corresponding individual compliances. This issue can be accounted for in our study by using a more conservative condition ($\text{cond } \mathcal{F} > M$, where M is a positive number that depends on data uncertainty) to define nonuniqueness.

The main significance of this work, however, is in establishing the limits of seismic fracture-characterization algorithms and identifying the class of fractured models which merits further investigation. Therefore, our results can provide a road map for future applications of seismic methodologies to naturally fractured reservoirs.

ACKNOWLEDGMENTS

We are grateful to members of the A(nisotropy)-Team of the Center for Wave Phenomena (CWP), Colorado School of Mines, for helpful discussions and to Roel Snieder and Reynaldo Cardona (both CSM) for their reviews of the manuscript. We also thank R. Cardona for providing Figure 1. This work was supported by the Consortium Project on Seismic Inverse Methods for Complex Structures at CWP and by the Chemical Sciences, Geosciences, and Biosciences Division, Office of Basic Energy Sciences, U.S. Department of Energy.

REFERENCES

- Angerer, E., Horne, S. A., Gaiser, J. E., Walters, R., Bagala, S., and Vetri, L., 2002, Characterization of dipping fractures using PS mode-converted data: 72nd Ann. Internat. Mtg., Soc. Expl. Geophys., Expanded Abstracts, 1010–1013.
- Bakulin, A., Grechka, V., and Tsvankin, I., 2000a, Estimation of fracture parameters from reflection seismic data—Part I: HTI model due to a single fracture set: *Geophysics*, **65**, 1788–1802.
- 2000b, Estimation of fracture parameters from reflection seismic data—Part II: Fractured models with orthorhombic symmetry: *Geophysics*, **65**, 1803–1817.
- 2000c, Estimation of fracture parameters from reflection seismic data—Part III: Fractured models with monoclinic symmetry: *Geophysics*, **65**, 1818–1830.
- 2002, Seismic inversion for the parameters of two orthogonal fracture sets in a VTI background medium: *Geophysics*, **67**, 289–296.
- Bakulin, A., Slater, C., Bunain, H., and Grechka, V., 2000d, Estimation of azimuthal anisotropy and fracture parameters from multi-azimuthal walkaway VSP in the presence of lateral heterogeneity: 70th Ann. Internat. Mtg., Soc. Expl. Geophys., Expanded Abstracts, 1405–1408.
- Berg, E., Hood, J., and Fryer, G., 1991, Reduction of the general fracture compliance matrix Z to only five independent elements: *Geophys. J. Internat.*, **107**, 703–707.
- Dewangan, P., and Grechka, V., 2002, Inversion of multicomponent, multi-azimuth, walkaway VSP data for the stiffness tensor: 72nd Ann. Internat. Mtg., Soc. Expl. Geophys., Expanded Abstracts, 161–164.
- Grechka, V., and Tsvankin, I., 2002, PP+PS=SS: *Geophysics*, **67**, 1961–1971.
- 2003, Characterization of dipping fractures in transversely isotropic background: *Geophys. Prosp.*, in press.
- Grechka, V., Bakulin, A., and Tsvankin, I., 2003, Seismic characterization of vertical fractures described as linear slip interfaces: *Geophys. Prosp.*, **51**, 117–130.
- Grechka, V., Contreras, P., and Tsvankin, I., 2000, Inversion of normal moveout for monoclinic media: *Geophys. Prosp.*, **48**, 577–602.
- Grechka, V., Pech, A., and Tsvankin, I., 2002, Multicomponent stacking-velocity tomography for transversely isotropic media: *Geophysics*, **67**, 1564–1574.
- Grechka, V., Theophanis, S., and Tsvankin, I., 1999, Joint inversion of P- and PS-waves in orthorhombic media: Theory and a physical-modeling study: *Geophysics*, **64**, 146–161.
- Grimm, R. E., Lynn, H. B., Bates, C. R., Phillips, D. R., Simon, K. M., and Beckham, W. E., 1999, Detection and analysis of naturally fractured gas reservoirs: Multi-azimuth seismic surveys in the Wind River basin, Wyoming: *Geophysics*, **64**, 1277–1292.
- Horne, S., and Leaney, S., 2000, Polarization and slowness component inversion for TI anisotropy: *Geophys. Prosp.*, **48**, 779–788.
- Lynn, H. B., Beckham, W. E., Simon, K. M., Bates, C. R., Layman, M., and Jones, M., 1999, P-wave and S-wave azimuthal anisotropy at a naturally fractured gas reservoir, Bluebell-Altamont field, Utah: *Geophysics*, **64**, 1312–1328.
- Nakagawa, S., Nihei, K. T., and Myer, L. R., 2000, Shear-induced conversion of seismic wave across single fractures: *Internat. J. Rock Mech. and Mining Sci.*, **37**, 203–218.
- Nichols, D., Muir, F., and Schoenberg, M., 1989, Elastic properties of rocks with multiple sets of fractures: 59th Ann. Internat. Mtg., Soc. Expl. Geophys., Expanded Abstracts, 471–474.
- Pérez, M. A., Grechka, V., and Michelena, R. J., 1999, Fracture detection in a carbonate reservoir using a variety of seismic methods: *Geophysics*, **64**, 1266–1276.
- Schoenberg, M., 1980, Elastic wave behavior across linear slip interfaces: *J. Acoust. Soc. Am.*, **68**, 1516–1521.
- 1983, Reflection of elastic waves from periodically stratified media with interfacial slip: *Geophys. Prosp.*, **31**, 265–292.

- Schoenberg, M., and Douma, J., 1988, Elastic wave propagation in media with parallel fractures and aligned cracks: *Geophys. Prosp.*, **36**, 571–590.
- Schoenberg, M., and Helbig, K., 1997, Orthorhombic media: Modeling elastic wave behavior in vertically fractured earth: *Geophysics*, **62**, 1954–1974.
- Schoenberg, M., and Muir, F., 1989, A calculus for finely layered anisotropic media: *Geophysics*, **54**, 581–589.
- Schoenberg, M., and Sayers, C., 1995, Seismic anisotropy of fractured rock: *Geophysics*, **60**, 204–211.
- Schoenberg, M., Dean, S., and Sayers, C. M., 1999, Azimuth-dependent tuning of seismic waves reflected from fractured reservoirs: *Geophysics*, **64**, 1160–1171.

- Tsvankin, I., 1997, Anisotropic parameters and P-wave velocity for orthorhombic media: *Geophysics*, **62**, 1292–1309.
- 2001, Seismic signatures and analysis of reflection data in anisotropic media: Elsevier Science Publ. Co., Inc.
- Tsvankin, I., and Grechka, V., 2000a, Dip moveout of converted waves and parameter estimation in transversely isotropic media: *Geophys. Prosp.*, **48**, 257–292.
- 2000b, Two approaches to anisotropic velocity analysis of converted waves: 70th Ann. Internat. Mtg., Soc. Expl. Geophys., Expanded Abstracts, 1193–1196.
- Winterstein, D. F., 1990, Velocity anisotropy terminology for geophysicists: *Geophysics*, **55**, 1070–1088.

APPENDIX A

COMPLIANCE MATRIX OF A GENERAL, ARBITRARILY ORIENTED FRACTURE SET

Here, we give exact expressions for the compliance matrix s_f of a set of general (e.g., microcorrugated) fractures with arbitrary orientation. The fracture planes are orthogonal to the unit vector \mathbf{n} defined by the azimuth α and dip β in the Cartesian coordinate frame $\{x_1, x_2, x_3\}$ (Figure 2):

$$\mathbf{n} = \{\cos \alpha \cos \beta, \sin \alpha \cos \beta, -\sin \beta\}. \quad (\text{A-1})$$

To obtain s_f , we apply an appropriate rotation to the compliance matrix s_f^{GN,x_1} [equation (5)] of a general fracture set orthogonal to the x_1 -axis ($\mathbf{n}^{x_1} = \{1, 0, 0\}$). This operation includes two steps—the rotation \mathbf{A}^β by the angle β around the x_2 -axis and another rotation \mathbf{A}^α by the angle α around the x_3 -axis—and is described by the matrix

$$\begin{aligned} \mathbf{A} &= \mathbf{A}^\alpha \mathbf{A}^\beta \\ &= \begin{pmatrix} \cos \alpha & -\sin \alpha & 0 \\ \sin \alpha & \cos \alpha & 0 \\ 0 & 0 & 1 \end{pmatrix} \begin{pmatrix} \cos \beta & 0 & \sin \beta \\ 0 & 1 & 0 \\ -\sin \beta & 0 & \cos \beta \end{pmatrix} \\ &= \begin{pmatrix} \cos \alpha \cos \beta & -\sin \alpha & \cos \alpha \sin \beta \\ \sin \alpha \cos \beta & \cos \alpha & \sin \alpha \sin \beta \\ -\sin \beta & 0 & \cos \beta \end{pmatrix}. \quad (\text{A-2}) \end{aligned}$$

The corresponding transformation of the compliance matrix s_f^{GN,x_1} (known as the Bond transformation) has the form

$$\mathbf{s}_f = \mathbf{B} \mathbf{s}_f^{\text{GN},x_1} \mathbf{B}^T. \quad (\text{A-3})$$

An explicit expression for the 6×6 matrix \mathbf{B} in terms of the elements of the matrix \mathbf{A} is given in Winterstein (1990); \mathbf{B}^T denotes the transposed matrix. Evaluating equation (A-3) yields the following 6×6 symmetric matrix \mathbf{s}_f :

$$\begin{aligned} s_{11f} &= \cos^2 \alpha \cos^2 \beta [K_H \sin^2 \alpha - \sin 2\alpha (K_{NH} \cos \beta \\ &\quad + K_{VH} \sin \beta) + \cos^2 \alpha (K_N \cos^2 \beta \\ &\quad + 2K_{NV} \sin 2\beta + K_V \sin^2 \beta)], \quad (\text{A-4}) \end{aligned}$$

$$\begin{aligned} s_{12f} &= \cos \alpha \cos^2 \beta \sin \alpha [\cos 2\alpha (K_{NH} \cos \beta \\ &\quad + K_{VH} \sin \beta) + \cos \alpha \sin \alpha (K_N \cos^2 \beta \\ &\quad + 2K_{NV} \sin 2\beta + K_V \sin^2 \beta - K_H)], \quad (\text{A-5}) \end{aligned}$$

$$\begin{aligned} s_{13f} &= \cos \alpha \cos \beta \sin \beta \{ \sin \alpha (K_{VH} \cos \beta - K_{NH} \sin \beta) \\ &\quad - \cos \alpha [K_{NV} \cos 2\beta + (K_V - K_N) \sin \beta \cos \beta] \}, \quad (\text{A-6}) \end{aligned}$$

$$\begin{aligned} s_{14f} &= \cos \alpha \cos \beta \{ -\cos^2 \alpha \sin \beta (K_{NH} \cos \beta \\ &\quad + K_{VH} \sin \beta) + \sin \alpha \cos \alpha [K_{NV} \cos 3\beta \\ &\quad + \sin \beta (K_H - K_N + (K_V - K_N) \cos 2\beta)] \\ &\quad + \sin^2 \alpha (K_{NH} \sin 2\beta - K_{VH} \cos 2\beta) \}, \quad (\text{A-7}) \end{aligned}$$

$$\begin{aligned} s_{15f} &= \cos \alpha \cos \beta \{ \cos \alpha \cos \beta \sin \alpha (3K_{NH} \sin \beta \\ &\quad - K_{VH} \cos \beta) + \cos^2 \alpha [K_{NV} \cos 3\beta \\ &\quad - \sin \beta (K_N + (K_N - K_V) \cos 2\beta)] \\ &\quad + \sin \beta (K_{VH} \sin 2\alpha \sin \beta - K_H \sin^2 \alpha) \}, \quad (\text{A-8}) \end{aligned}$$

$$\begin{aligned} s_{16f} &= \cos \alpha \cos^2 \beta [K_H \sin^3 \alpha + \cos \alpha (1 - 4 \sin^2 \alpha) \\ &\quad \times (K_{NH} \cos \beta + K_{VH} \sin \beta) + \cos^2 \alpha \sin \alpha \\ &\quad \times (2K_N \cos^2 \beta + 2K_{NV} \sin 2\beta + 2K_V \sin^2 \beta - K_H)], \quad (\text{A-9}) \end{aligned}$$

$$\begin{aligned} s_{22f} &= \cos^2 \beta \sin^2 \alpha (K_H \cos^2 \alpha + K_N \cos^2 \beta \sin^2 \alpha \\ &\quad + K_{NH} \cos \beta \sin 2\alpha + K_{VH} \sin 2\alpha \sin \beta \\ &\quad + K_V \sin^2 \alpha \sin^2 \beta + K_{NV} \sin^2 \alpha \sin 2\beta), \quad (\text{A-10}) \end{aligned}$$

$$\begin{aligned} s_{23f} &= \cos \beta \sin \alpha \sin \beta \{ \cos \alpha (K_{NH} \sin \beta - K_{VH} \cos \beta) \\ &\quad - \sin \alpha [K_{NV} \cos 2\beta + (K_V - K_N) \sin \beta \cos \beta] \}, \quad (\text{A-11}) \end{aligned}$$

$$\begin{aligned} s_{24f} &= \frac{\cos \beta \sin \alpha}{4} \{ 4K_{NV} \cos 3\beta \sin^2 \alpha - 4 \sin \beta \\ &\quad \times [K_H \cos^2 \alpha + K_N \sin^2 \alpha + (K_N - K_V) \\ &\quad \times \sin^2 \alpha \cos 2\beta] + \sin 2\alpha (3K_{VH} \cos 2\beta \\ &\quad - 3K_{NH} \sin 2\beta - K_{VH}) \}, \quad (\text{A-12}) \end{aligned}$$

$$\begin{aligned} s_{25f} &= \cos \beta \sin \alpha \{ \sin \alpha \sin \beta [K_H \cos \alpha + (K_{NH} \cos \beta \\ &\quad + K_{VH} \sin \beta) \sin \alpha] - 2 \cos \alpha \cos \beta \sin \beta \\ &\quad \times [K_{NH} \cos \alpha + (K_N \cos \beta + K_{NV} \sin \beta) \sin \alpha] \\ &\quad + \cos \alpha \cos 2\beta [K_{VH} \cos \alpha + (K_{NV} \cos \beta \\ &\quad + K_V \sin \beta) \sin \alpha] \}, \quad (\text{A-13}) \end{aligned}$$

$$\begin{aligned} s_{26f} &= \cos^2 \beta \sin \alpha \{ \sin \alpha (4 \cos^2 \alpha - 1) (K_{NH} \cos \beta \\ &\quad + K_{VH} \sin \beta) - \cos \alpha \sin^2 \alpha [K_H - K_N - K_V \\ &\quad + (K_V - K_N) \cos 2\beta - 2K_{NV} \sin 2\beta] + K_H \cos^3 \alpha \}, \quad (\text{A-14}) \end{aligned}$$

$$s_{33f} = \sin^2 \beta (K_V \cos^2 \beta - K_{NV} \sin 2\beta + K_N \sin^2 \beta), \quad (\text{A-15})$$

$$s_{34f} = -\sin \beta \{ K_V \cos^3 \beta \sin \alpha - 3K_{NV} \cos^2 \beta \sin \alpha \sin \beta + \sin^2 \beta (K_{NH} \cos \alpha + K_{NV} \sin \alpha \sin \beta) - \cos \beta \sin \beta [K_{VH} \cos \alpha + (K_V - 2K_N) \times \sin \alpha \sin \beta] \}, \quad (\text{A-16})$$

$$s_{35f} = -\sin \beta \{ \sin \alpha \sin \beta (K_{VH} \cos \beta - K_{NH} \sin \beta) + \frac{\cos \alpha}{2} [(K_V + K_N) \cos \beta + (K_V - K_N) \cos 3\beta - 2K_{NV} \sin 3\beta] \}, \quad (\text{A-17})$$

$$s_{36f} = \sin \beta \cos \beta \{ \cos 2\alpha (K_{NH} \sin \beta - K_{VH} \cos \beta) - \sin 2\alpha [K_{NV} \cos 2\beta + (K_V - K_N) \sin \beta \cos \beta] \}, \quad (\text{A-18})$$

$$s_{44f} = K_V \cos^4 \beta \sin^2 \alpha - 4K_{NV} \cos^3 \beta \sin^2 \alpha \sin \beta + 4 \cos \beta \sin \alpha \sin^2 \beta (K_{NH} \cos \alpha - K_{NV} \sin \alpha \sin \beta) - 2 \cos^2 \beta \sin \alpha \sin \beta [K_{VH} \cos \alpha + (K_V - 2K_N) \times \sin \alpha \sin \beta] + \sin^2 \beta [K_H \cos^2 \alpha + (K_{VH} \sin 2\alpha + K_V \sin^2 \alpha \sin \beta) \sin \beta], \quad (\text{A-19})$$

$$s_{45f} = -\cos 2\alpha \sin \beta (K_{VH} \cos 2\beta - K_{NH} \sin 2\beta) - \frac{\sin 2\alpha}{4} [K_V + K_N + (K_V - K_N) \cos 4\beta - 2K_H \sin^2 \beta - 2K_{NV} \sin 4\beta], \quad (\text{A-20})$$

$$s_{46f} = \cos \beta \{ \cos 2\alpha [K_{VH} \cos^2 \beta \sin \alpha - 2K_{NH} \cos \beta \sin \alpha \sin \beta - \sin \beta (K_H \cos \alpha + K_{VH} \sin \alpha \sin \beta)] - 2 \cos \alpha \sin \alpha [(2K_N - K_V) \times \cos^2 \beta \sin \alpha \sin \beta - K_{NV} \cos^3 \beta \sin \alpha + \cos \beta \sin \beta (K_{NH} \cos \alpha + 3K_{NV} \sin \alpha \sin \beta) + \sin^2 \beta (K_{VH} \cos \alpha + K_V \sin \alpha \sin \beta)] \}, \quad (\text{A-21})$$

$$s_{55f} = -\sin 2\alpha \sin^2 \beta (2K_{NH} \cos \beta + K_{VH} \sin \beta) + \sin \beta (K_{VH} \cos^2 \beta \sin 2\alpha + K_H \sin^2 \alpha \sin \beta) + \frac{\cos^2 \alpha}{2} [K_V + K_N + (K_V - K_N) \cos 4\beta - 2K_{NV} \sin 4\beta], \quad (\text{A-22})$$

$$s_{56f} = \cos \beta \{ K_H \cos 2\alpha \sin \alpha \sin \beta + \cos^2 \alpha \sin \alpha \times [2K_{NV} \cos 3\beta - 2(K_N + (K_N - K_V) \cos 2\beta) \times \sin \beta] + \cos \alpha [2 \sin^2 \alpha \sin \beta (K_{NH} \cos \beta + K_{VH} \sin \beta) + \cos 2\alpha (K_{VH} \cos 2\beta - K_{NH} \sin 2\beta)] \}, \quad (\text{A-23})$$

$$s_{66f} = \cos^2 \beta \{ K_H (\cos^4 \alpha + \sin^4 \alpha) + 2 \sin 2\alpha (K_{NH} \cos \beta + K_{VH} \sin \beta) - \frac{\sin^2 2\alpha}{2} [K_H - K_N - K_V + (K_V - K_N) \cos 2\beta - 2K_{NV} \sin 2\beta] \}. \quad (\text{A-24})$$

Equations (A-4)–(A-24) are derived for the most general fracture rheology described by six independent excess fracture compliances. The matrices s_f for diagonal [equation (7)] or rotationally invariant [equation (9)] fractures can be obtained by substituting the corresponding constraints (8) and (10).